[7] K. G. Wilson and M. E. Fisher, Phys. Rev. Lett. 28, 240 (1972).

[8] K. G. Wilson, Phys. Rev. Lett. 28, 548 (1972).

[9] See S. Ma, Phys. Rev. A 7, 2172 (1973); R. Abe, Progr. Theor. Phys. 49, 113 (1973).

[10] A. Aharony, to be published; R. Abe and S. Hikami, Progr. Theor. Phys. 49, 442 (1973).

[11] See references cited in Fisher, Refs. 1 and 2; Kadanoff, Ref. 3; by P. Heller, Rep. Progr. Phys. 30, 731 (1967); J. Als-Nielsen and O. Dietrich, Phys. Rev. 153, 706, 711, 717 (1969); J. Als-Nielsen, Phys. Rev. 185, 664 (1969); D. Bally, M. Popovici, M. Totia, B. Grabcev, and A. M. Lungu, Phys. Lett. 26A, 396 (1968); J. Als-Nielsen, Phys. Rev. Lett. 25, 730 (1970); M. Popovici, Phys. Lett. 34A, 319 (1971).

[12] Als-Nielsen and Dietrich, Ref. 11; Als-Nielsen, Ref. 11.

[13] Bally, Popovici, Totia, Grabcev, and Lungu, Ref. 11; Als-Nielsen, Ref. 11; Popovici, Ref. 11.

[14] M. A. Moore, D. Jasnow, and M. Wortis, Phys. Rev. Lett. 22, 940 (1972).

[15] M. Ferer, M. A. Moore, and M. Wortis, Phys. Rev. Lett. 22, 1382 (1969) [the apparent failure of scaling found here for $E_1(r)$ may well be due to the relatively small values of r/a sampled], and Phys. Rev. B 3, 3911 (1971); M. Ferer, Phys. Rev. B 4, 3964 (1971); M. Ferer and M. Wortis, Phys. Rev. B 6, 3426 (1972).

[16] Ritchie and Fisher, Ref. 1; Tarko and Fisher, Ref. 1.

[17] E. Brézin, D. J. Wallace, and K. G. Wilson, Phys. Rev. Lett. 29, 591 (1972), and Phys. Rev. B 7, 232 (1973); E. Brézin and D. J. Wallace, Phys. Rev. B 7, 1967 (1973).

[18] G. M. Avdeeva and A. A. Migdal, Pis'ma Zh. Eksp. Teor. Fiz. 16, 253 (1972) [JETP Lett. 16, 178 (1972)].

[19] See Refs. 1, 4, 15, and 16 in M. E. Fisher, in *Critical Phenomena,* edited by M. S. Green and J. V. Sengers, National Bureau of Standards Miscellaneous Publication No. 273 (U.S. GPO, Washington, D.C., 1966), p. 108; M. E. Fisher and J. S. Langer, Phys. Rev. Lett. 20, 665 (1968). A general argument can also be based on the operator-product expansion: L. P. Kadanoff, Phys. Rev. Lett. 23, 1430 (1969); K. G. Wilson, Phys. Rev. 179, 1499 (1969), and Phys. Rev. D 2, 1473 (1970). Recently E. Brézin, D. J. Amit, and J. Zinn-Justin, to be published, have presented a formal derivation based on the operator-product expansion and the Callan-Symanzik equation which shows, particularly, the origin of the term linear in t.

[20] Fisher and Langer, Ref. 19.

[21] Full details of the calculation will be published elsewhere.

[22] This step assumes the scaling relation $(2-\eta)\nu=\gamma$ which, however, is explicitly confirmed through the coefficient $\frac{1}{8}$ in Eq. (24). See also D. J. Amit, Phys. Lett. 42A, 299 (1972); Abe and Hikami, Ref. 10.

Experimental Observation of the Nonoscillatory Parametric Instability at the Lower-Hybrid Frequency

R. P. H. Chang
Bell Laboratories, Murray Hill, New Jersey 07974

and

M. Porkolab
Plasma Physics Laboratory, Princeton University, Princeton, New Jersey 08540

(Received 7 August 1973)

The nonoscillatory parametric instability is observed when the "pump" frequency is near the lower-hybrid frequency. Strong heating of both the ions and electrons has also been measured.

Although predicted by theory,[1] to our knowledge the nonoscillatory parametric instability (the oscillating two-stream instability or the purely growing mode) has not yet been verified experimentally. Some of the reasons for the difficulty of observing such modes are the following: (a) The oscillatory decay instability has a lower threshold in most cases of interest than the nonoscillatory instability; thus it tends to "cover up" the possible presence of the latter.[1] (b) Spectral analysis and wavelength measurements are very difficult since the real part of the frequency for the purely growing mode is zero. Recently it has been shown, however, that for pump frequencies very near the lower-hybrid frequency the threshold for the oscillatory parametric decay instability increases rapidly.[2] The reason for such increase in the threshold is that the wave-vector matching condition produces considerable electron Landau damping of the ion acoustic waves with frequencies above the ion-cyclotron frequency, and/or prevents such a coupling altogether[2] (with the possible exception of the ion-cyclotron mode[3]). In addition, parametric decay into ion acoustic waves with frequencies below the ion-cyclotron frequency may often be prevented by ion-neutral or ion-ion collisions in typical laboratory plasmas.[4] On the contrary, it has been shown that ion collisional damping does not affect the threshold for decay into the nonoscillatory mode.[1,2,5] The threshold has been given[2,5,6] for decay into the nonoscillatory mode with the pump frequency

$$\omega_0 = \omega_{LH}(1 + k_z^2 M_i/k^2 m_e)^{1/2} \tag{1}$$

near the lower-hybrid frequency $\omega_{LH} \equiv \omega_{pi}/(1 + \omega_{pe}^2/\Omega_e^2)^{-1/2}$ (here ω_{pj} and Ω_j are jth-species plasma frequency and gyrofrequency, respectively). We recall that in this decay process the $\vec{E}_{rf} \times \vec{B}_0$ force drives the instability so that the waves propagate almost orthogonally to the applied rf pump electric field $E_{rf}\hat{y}$ and the static confining magnetic field $B_0\hat{z}$. In order to ascertain that no other instability can exist in our experimental regime, we have solved numerically the complete parametric dispersion relationship including ion-ion, ion-neutral, and electron-neutral collisions, as well as Landau damping.[4] The results showed that (in the regime $\omega \ll \omega_{ci}$)under the present experimental conditions there were no unstable roots other than the zero-frequency mode.

Thus, we have undertaken an experimental search for the nonoscillatory parametric instability for pump frequencies in the vicinity of the lower-hybrid frequency, and we wish to report here what we believe to be the first experimental confirmation of such an instability. In order to overcome the difficulties presented in point (b), we have installed a series of hot filaments (for emitting additional electrons) across the plasma column (see Fig. 1). By varying the electron emission of each filament, we can change the dc electric field $\vec{E}_{dc}$ (in the direction of $\vec{E}_{rf}$ but perpendicular to $\vec{B}_0$) in the plasma in a controlled manner. In the present case such a dc electric field produced an $\vec{E}_{dc} \times \vec{B}_0$ drift velocity (in the direction of the parametrically excited waves) which Doppler shifts the frequencies of all the modes in a parametric process, but does not affect the stability of the system.[7] Thus, one can shift the "frequency" of the purely growing mode ($\omega_R = 0$) in the lab frame of reference into an observable regime (i.e., $\omega_R = \vec{k}\cdot C\vec{E}_{dc} \times \vec{B}_0/B_0^2$), and one can perform wavelength and spectrum measurements. In addition to verifying the fundamental properties of the nonoscillatory mode, we have also measured enhanced plasma heating of both the electrons and ions when the pump frequency is near the lower-hybrid frequency. We expect that this anomalous heating may play an important role in the rf heating of fusion plasmas.[8,9]

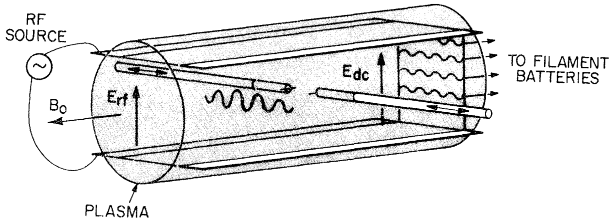

FIG. 1. Simplified schematic of the experimental setup. A set of plates for rf field coupling was immersed in the plasma. Parametrically excited waves were measured using the set of coaxial probes. Electron emission from each filament could be controlled individually to provide the desired E_{dc}. The axial probe, Langmuir probe, multigrid energy analyzers, and other rf probes used in the experiment are not shown here.

The experiments were performed in a plasma which was produced by a hot-cathode discharge at one end of a linear plasma device.[10] The plasma column was 200 cm long and approximately 14 cm in diameter (with a substantially uniform region of 6 cm in diameter). A large and uniform plasma was needed for this experiment since the lower-hybrid frequency is proportional to the square root of the density. With this uniform plasma we can also eliminate the possible occurrence of drift waves. Hydrogen as well as noble gases (He, Ne, Ar) were used in these experiments. Typical plasma parameters were as follows: density $N_0 = 10^{10}-3\times 10^{10}$ cm^{-3}; magnetic field $B_0 \leq 500$ G; collision frequencies—ion-neutral, $\nu_{i0} \simeq 5\times 10^4$ sec^{-1}, electron-neutral, $\nu_{e0} \simeq 3\times 10^6$ sec^{-1}; electron temperature $T_e = 3-7$ eV, and ion temperature $T_i \leq 0.1$ eV for the gases used. A simplified schematic of the experimental setup is shown in Fig. 1. The external driving field was coupled to the plasma via a set of symmetrically driven plates immersed in the plasma. The plates were 100 cm long by 13 cm wide and spaced 9 cm apart. The pump frequency was varied from 5 to 200 MHz. Wavelength and frequency measurements were carried out by means of shielded high-frequency probes, which could travel along and across the magnetic field lines. Energy distributions for the electrons and ions were measured by means of two multigrid energy analyzers. In what follows, experimental results obtained mostly from a hydrogen plasma will be presented. Similar results have also been obtained from other gases mentioned above.

By coupling to the plasma an rf signal just above the lower-hybrid frequency $f_0 = 30$ MHz, typical parametric decay spectra such as shown in Fig. 2(a), top, were observed above a certain threshold of the pump field. Here we notice the presence of a band of low-frequency signals (believed to be the Doppler-shifted purely growing modes), and the Doppler-shifted sidebands around the pump frequency. Notice that most of the signal is below the ion-cyclotron frequency (687 kHz). This continuum spread of sideband and low-frequency signals comes about because of the lower-hybrid dispersion relationship [i.e., $\omega \propto k_\parallel/k$, Eq. (1)]. The width of the spread is determined by the amount of Landau damping on the waves.[4,5] The enhancement of the signal at $f = 17$ kHz and the corresponding sideband signals are believed to be due to finite-plasma effects. This fact is borne out from wavelength measurements described below. To ascertain the presence of Doppler shift, we have varied the dc electric field strength between the driving plates and observed a corresponding linear frequency shift (the other plasma parameters were kept constant). A plot of the measured decay frequencies (using the $f = 17$ kHz mode and its wavelength) versus the measured dc electric field strengths in the plasma is shown in Fig. 2(b). The solid line gives the $\vec{E}_{dc} \times \vec{B}_0$ Doppler-shifted frequency, where the measured wavelength and electric field strengths were used. Notice that as E_{dc} approaches zero, the real part of the frequency vanishes, thus verifying the presence of the purely growing mode. By reversing the direction of the drift, we obtained the same results. The wavelengths were measured with the movable probes and a radio interferometer (with narrow-band-pass filters).[10] The wavelengths for the Doppler-shifted zero-frequency mode ($f = 17$ kHz) and the corresponding sidebands are approximately 5 cm, which is comparable to the uniform cross section of the plasma. Typical examples of interferometer outputs (from an x-y recorder) are shown in Fig. 3 (for $f = 34$ kHz and corresponding

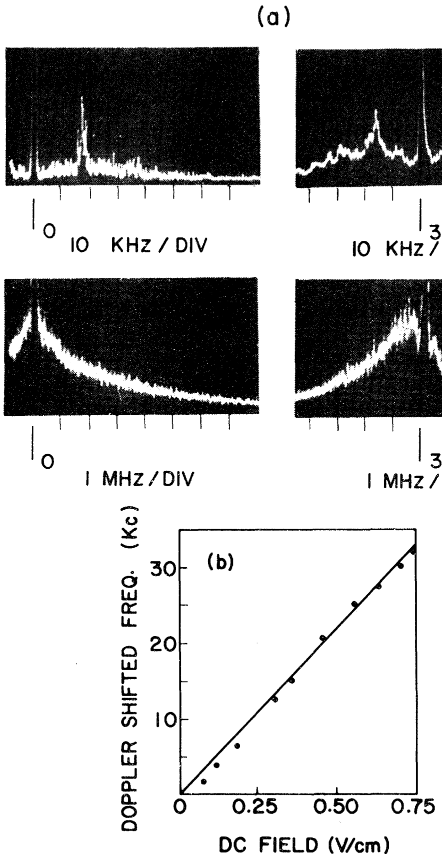

FIG. 2. (a) Top: spectra just above threshold for instability. Doppler-shifted purely growing modes (left-hand side) and Doppler-shifted lower-hybrid sideband modes (right-hand side). Bottom: spectra for rf power 100 times that above threshold. (b) A plot of the measured Doppler-shifted zero frequency versus the measured dc field. The solid line gives the $\vec{E}_{dc} \times \vec{B}_0$ Doppler-shifted frequency for a measured wavelength of 5 cm and a magnetic field of 450 G.

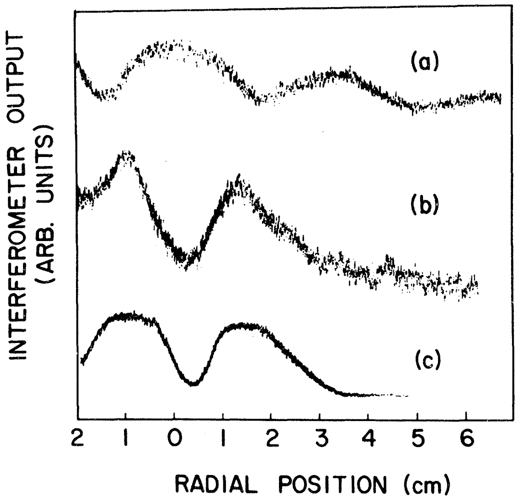

FIG. 3. Typical interferometer traces of a Doppler-shifted lower sideband (curve *a*), upper sideband (curve *b*), and frequency mode (curve *c*).

sidebands). The distortion of the sinusoidal interference patterns is believed to be due to the spread of wave numbers about the most unstable one for a given frequency.[4] The direction of k for the perpendicular waves was found to be orthogonal to the rf pump field and the dc magnetic field, in agreement with an $\vec{E}_{nb}\times\vec{B}_0$ driving mechanism. From the density-profile measurements and a mapping of the wave amplitudes using the spectrum analyzer, we found that the amplitudes were maximum near the center of the plasma column. Wavelengths along the magnetic field were also measured. For $f=17$ kHz they were found to be 200 cm (comparable to the machine length). Using the measured plasma parameters we have identified the sidebands as Doppler-shifted lower-hybrid waves which satisfied Eq. (1). From the frequency and wavelength measurements we conclude that the corresponding frequency and wave-number selection rules are satisfied. The threshold electric fields were measured with calibrated rf probes, and were determined from semilog plots of the excited modes versus the pump power.[10] For the modes measured above we found $E_{\text{expt}}\cong 3$ V/cm (with an uncertainty of a factor of 2), in agreement with the theoretical value (for the case of infinite plasma) of $E_{\text{theor}}=4.5$ V/cm.[4] This threshold field corresponds to $\vec{E}_{\text{rf}}\times\vec{B}_0$ drift velocity of approximately half the ion acoustic speed.

As the pump-field strength was increased to 20 V/cm, we observed broadening of the spectrum [see bottom spectra in Fig. 2(a); higher-frequency components also appeared ($\omega>\omega_{ci}$)] and at the same time plasma heating took place. A factor-of-4 increase in the electron temperature was measured both by a Langmuir probe and a multigrid energy analyzer. An extra thin (3 mm thick) multigrid energy analyzer (with the grid surface aligned along the magnetic field lines) was used to measure energetic ions. We measured Maxwellian distribution of energetic ions from a few volts to nearly a hundred volts. A typical heating time of 5–10 μsec was also measured. The excitation of the higher-frequency components $\omega>\omega_{ci}$ and the plasma heating are presently under detailed study.

In conclusion, we have observed nonoscillatory parametric instability near the lower-hybrid resonant frequency. Measurements of the threshold fields and wavelengths associated with this instability have been made and compared with theory. This instability may play an important role in rf heating of fusion plasmas near the lower-hybrid frequency.[9]

We are grateful to L. N. Pfeiffer who has kindly lent us his rf amplifier for this experiment. We thank T. E. Adams for technical assistance. Interest shown by A. Hasegawa, W. L. Brown, and J. A. Giordmaine is appreciated.

---

[1] K. J. Nishikawa, J. Phys. Soc. Jap. 24, 916, 1152 (1968). Kim *et al.* have shown some preliminary evidence pointing toward the possible presence of a nonoscillatory parametric instability in a double-plasma device [H. C. Kim *et al.*, Bull. Amer. Phys. Soc. 17, 1060 (1972)].

[2] M. Porkolab, in *Proceedings of the Symposium on Plasma Heating and Injection, Varenna, Italy, 1972* (Editrice Compositori, Bologna, Italy, 1973), p. 46.

[3] Recently, Chu *et al.* observed plasma heating due to parametrically driven ion-cyclotron modes in a Q-machine plasma with $T_i\geq T_e$ [T. K. Chu *et al.*, Phys. Rev. Lett. 31, 211 (1973)].

[4] M. Porkolab and R. P. H. Chang, to be published.

[5] M. Porkolab, Nucl. Fusion 12, 329 (1972).

[6] J. M. Kindel, H. Okuda, and J. M. Dawson, Phys. Rev. Lett. 29, 995 (1972).

[7] This is true as long as the dc electric fields are sufficiently small so that the centrifugal forces associated with the plasma rotation are negligible. No instability due to applied dc electric fields was observed. A Langmuir probe was used to monitor the density profile to ensure that no gradients were formed when the dc field was present.

[8] T. H. Stix, Phys. Rev. Lett. 15, 878 (1965).

[9] V. M. Glagolev, N. A. Krivov, and Yu. V. Skosyrev, in *Proceedings of the Fourth International Conference on Plasma Physics and Controlled Nuclear Fusion Research, Madison, Wisconsin, 1971* (International Atomic Energy Agency, Vienna, 1971), Vol. II, 559.

[10] R. P. H. Chang and M. Porkolab, Phys. Fluids 13, 2766 (1970), and Phys. Rev. Lett. 28, 206 (1972).

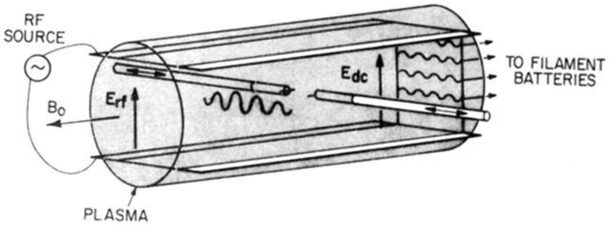

FIG. 1. Simplified schematic of the experimental setup. A set of plates for rf field coupling was immersed in the plasma. Parametrically excited waves were measured using the set of coaxial probes. Electron emission from each filament could be controlled individually to provide the desired E_{dc}. The axial probe, Langmuir probe, multigrid energy analyzers, and other rf probes used in the experiment are not shown here.

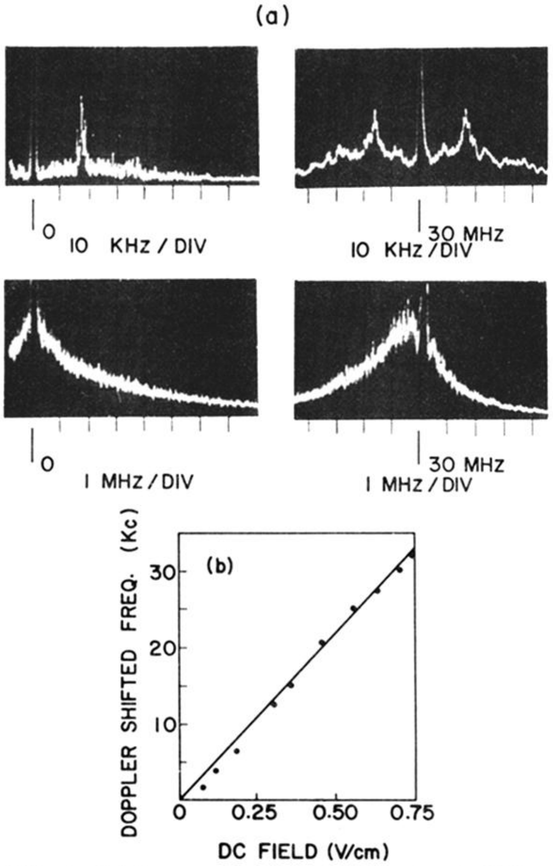

FIG. 2. (a) Top: spectra just above threshold for instability. Doppler-shifted purely growing modes (left-hand side) and Doppler-shifted lower-hybrid sideband modes (right-hand side). Bottom: spectra for rf power 100 times that above threshold. (b) A plot of the measured Doppler-shifted zero frequency versus the measured dc field. The solid line gives the $\vec{E}_{dc} \times \vec{B}_0$ Doppler-shifted frequency for a measured wavelength of 5 cm and a magnetic field of 450 G.